Published in final edited form as:
Ann Neurol. 2012 July ; 72(1): 76–81. doi:10.1002/ana.23566.

Functional MRI Detection of Vascular Reactivity in Cerebral Amyloid Angiopathy

Andrew Dumas, MA[1], **Gregory A Dierksen, M.Eng**[1], **M Edip Gurol, MD**[1], **Amy Halpin, BA**[1], **Sergi Martinez-Ramirez, MD**[1], **Kristin Schwab, BA**[1], **Jonathan Rosand, MD, Msc**[1], **Anand Viswanathan, MD, PhD**[1], **David H Salat, PhD**[2,3], **Jonathan R Polimeni, PhD**[3], and **Steven M Greenberg, MD, PhD**[1]

[1]Hemorrhagic Stroke Research Center, Department of Neurology, Massachusetts General Hospital, Harvard Medical School, Boston, MA USA

[2]Neuroimaging Research For Veterans Center, Boston VA Healthcare System, Department of Radiology, Massachusetts General Hospital, Harvard Medical School, Boston, MA USA

[3]Athinoula A. Martinos Center for Biomedical Imaging, Department of Radiology, Massachusetts General Hospital, Harvard Medical School, Boston, MA USA

Abstract

Objective—In addition to its role in hemorrhagic stroke, advanced cerebral amyloid angiopathy (CAA) is also associated with ischemic lesions and vascular cognitive impairment. We used functional MRI techniques to identify CAA-associated vascular dysfunction.

Methods—Functional MRI was performed on 25 nondemented subjects with probable CAA (mean ± standard deviation age 70.2±7.8) and 12 healthy elderly controls (age 75.3±6.2). Parameters measured were reactivity to visual stimulation (quantified as blood oxygen level-dependent [BOLD] response amplitude, time to peak response, and time to return to baseline after stimulus cessation) and resting absolute cerebral blood flow in the visually activated region (measured by arterial spin labeling).

Results—CAA subjects demonstrated reduced response amplitude (percent change in BOLD signal 0.65±0.28 vs 0.89±0.14, $p<0.01$), prolonged time to peak (11.1±5.1 vs 6.4±1.8 sec, $p<0.001$) and prolonged time to baseline (16.5±6.7 vs 11.6±3.1 sec, $p<0.001$) relative to controls. These differences were independent of age, sex, and hypertension in multivariable analysis and were also present in secondary analyses excluding nonresponsive voxels or voxels containing chronic blood products. Within the CAA group, longer time to peak correlated with overall volume of white matter T2 hyperintensity (Pearson correlation 0.53, $p=0.007$). Absolute resting blood flow in visual cortex, in contrast, was essentially identical between the groups (44.0±12.6 vs 45.0±10.0 ml/100g/min, $p=0.8$).

Interpretation—Functional MRI identifies robust differences in both amplitude and timing of the response to visual stimulation in advanced CAA. These findings point to potentially powerful approaches for identifying the mechanistic links between vascular amyloid deposits, vascular dysfunction, and CAA-related brain injury.

In addition to its role as a major cause of primary intracerebral hemorrhage, cerebrovascular deposition of the ß-amyloid peptide (cerebral amyloid angiopathy, CAA) also appears to cause ischemic brain injury. Advanced CAA is associated with various neuropathological or

Correspondence: Steven M. Greenberg, MD, PhD MGH Stroke Research Center 55 Fruit Street CPZ 175 Suite 300 Boston, MA 02114 617-724-1874 (phone) sgreenberg@partners.org.

neuroimaging markers of nonhemorrhagic tissue injury, including microinfarcts,[1–5] white matter lesions,[6, 7] and altered diffusion-tensor properties.[8] These multifocal lesions likely contribute to the association between advanced CAA and cognitive impairment observed in community-dwelling elderly individuals.[9]

Determining the mechanism of CAA-related ischemic injury would be an important step towards identifying candidate treatment approaches. One possibility suggested by studies in transgenic mouse models,[10–12] and human studies using functional transcranial Doppler (fTCD)[13, 14] is that CAA may reduce the ability of cerebral resistance vessels to dilate in response to physiologic stimulation. Impaired vasoreactivity might in turn cause mismatches between perfusion and metabolic demand, predisposing to ischemic damage.

The current analysis applies functional MRI (fMRI) to examine cerebrovascular reactivity and blood flow in patients diagnosed with advanced CAA. Functional MRI offers several important advantages over fTCD, including anatomic information on the location of impaired vasoreactivity and the ability to measure absolute blood flow using arterial spin labeling fMRI techniques. The current analysis focuses on the vascular properties of visually activated cortex, a brain region with high burdens of cerebrovascular amyloid in advanced CAA.[15–17]

Methods

Study populations and structural MRI

Structural and functional MRI was performed on 25 CAA subjects, recruited from an ongoing longitudinal study of CAA.[18] The CAA subjects met criteria for probable CAA[19] based on neuropathological samples (n=4) or presence of multiple strictly lobar hemorrhagic lesions (n=21). We also performed fMRI on 12 similar aged subjects without history of intracerebral hemorrhage. Control subjects were selected from among cognitively normal members of the National Alzheimer's Coordinating Center-based Uniform Dataset cohort at Massachusetts General Hospital. Demographic information, current medications, history of hypertension, diabetes, hyperlipidemia, or dementia, and current tobacco use were determined by patient interview and chart review as previously described.[2] Exclusion criteria for both groups were dementia, a diagnosis of cerebrovascular disease other than CAA, and contraindication to fMRI (metallic implant/devices, claustrophobia, seizure history). For subjects who underwent more than one fMRI session, the session with the least apparent head motion during the functional acquisition was analyzed. All participants provided informed consent for this study and all procedures were approved by the Massachusetts General Hospital Institutional Review Board.

Study participants underwent structural and functional scanning at 1.5T using a Siemens Avanto system (Siemens Healthcare, Erlangen, Germany) for each experimental session. Two T1-weighted sagittal scans (Multi-echo MPRAGE,[20] 1×1×1mm voxel size), T2*-weighted 2D axial images (1×1mm in-plane resolution, 5mm slice thickness, TR/TE 750/24msec) and FLAIR 3D axial images (1×1×1mm) were acquired using the vendor-supplied 12-channel head coil in the same scanning session used for fMRI. Microbleeds and macrobleeds were identified on the T2*-weighted images by a trained neurologist as described.[21] Volume of white matter hyperintensity on FLAIR sequences was determined by computer-assisted methods and corrected for head size as described,[7] yielding normalized white matter hyperintensity (nWMH) volumes.

fMRI image acquisition and analysis

The details of fMRI image acquisition, task design, and image processing are described in the Supplementary Methods. Briefly, BOLD-weighted echo-planar imaging (EPI) volumes

positioned on the occipital lobes were acquired using the vendor-supplied 32-channel coil. The visual stimulus consisted of 16 blocks of a 8-Hz flashing radial black-and-white checkerboard pattern for 20 seconds followed by 28 seconds of gray screen.

For CAA subjects without prior occipital ICH (n=21), both hemispheres were incorporated in the image analysis. For subjects with occipital tissue damage on the T1-weighted structural scan (n=4), the affected hemisphere was excluded from the analysis. Pre-processed functional volumes were co-registered to the multi-echo MPRAGE structural images as described[22] (and Supplementary Methods). A surface-based region of typical functional activation was identified on the mesh representation of the cerebral cortical surface using the first 8 control subjects scanned and 8 age- and gender-matched CAA subjects. The common functional ROI represented a single contiguous surface region of activation (Fig. 1a) demonstrating significant activation at an uncorrected threshold of $p<0.001$. The average time course of the BOLD response to the visual stimulus for each study participant was calculated by averaging the time-courses of all voxels within this ROI and converting to BOLD percent signal change using the time-course average as a baseline value, then averaging across the 16 stimulus blocks.

Subjects' block responses were fit to a trapezoidal function with parameters to describe the time to reach peak response, the response amplitude, and the time to return to baseline (see Supplementary Methods and Fig. 2b). Two secondary analyses were performed to address the possible role of CAA-related tissue damage in reducing the fMRI response. The first of these analyses used a more restrictive subset of the common functional ROI (selected by relatively conservative methods; see Supplementary Methods) to exclude non-responding voxels for each individual. The second of these analyses excluded all voxels containing evidence of hemorrhage on T2*-weighted sequences.

Arterial Spin Labeling (ASL) was performed using the Siemens PICORE Q2TIPS pulse sequence in the absence of visual stimulation to determine mean resting cerebral blood flow (CBF) in the functionally activated ROI. ASL was performed on 22 of the 25 CAA subjects and all 12 controls; it was omitted in 3 of the CAA subjects because of scan-related time constraints. Quantitative processing was performed as described.[23] Briefly, images were first motion-corrected and smoothed using a Gaussian FWHM of 5 voxels. The mean tag-control difference image was generated using surround subtraction and quantitative CBF values were generated according to the single-compartment Standard Kinetic Model. The functional ROI was used as a mask for the ASL data, and the mean CBF value calculated for the voxels within this mask.

Statistical analysis

Univariate comparisons of demographic, clinical, and fMRI parameters between CAA cases and control subjects were performed by t-test (for continuous variables) or Fisher's exact test (categorical variables). Within the CAA group, the fMRI parameters (time to peak, amplitude, time to baseline) were analyzed for correlation with number of microbleeds and nWMH by linear regression and Pearson correlation coefficient R. Time to peak, time to baseline, hemorrhagic lesion counts, and nWMH were log transformed for all statistical analyses to generate normal distributions. Multivariable analyses were performed to control for age, sex, hypertension, and use of antihypertensive agents (classified as calcium-channel blockers, beta blockers, or other antihypertensive agent, adding each separately to the multivariable models).

Results

We analyzed change in BOLD signal in response to visual stimulation in 25 nondemented patients diagnosed with probable CAA and 12 elderly nondemented control subjects. The CAA patients (Table 1) were approximately 5 years younger than the controls, had slightly lower scores on the Mini-Mental State Examination, a nonsignificant ($p>0.1$) trend towards more hypertension, and similar proportions of hyperlipidemia, diabetes mellitus or tobacco use. Comparison of fMRI responses to visual stimulation demonstrated significantly lower amplitude of response (Fig. 1b), longer time to reach peak response, and longer time to return to baseline after discontinuation of the visual stimulus in CAA subjects relative to controls (Table 2, Fig. 2). These differences were independent of age, sex, hypertension, and use of antihypertensive agent in multivariable analysis. The amplitude of undershoot of the baseline during the stimulus-off interval did not differ between CAA and controls.

To exclude the possibility that differences between CAA and control subjects were driven by CAA-related structural damage (even without hemorrhagic stroke), we performed a secondary analysis restricted to those voxels in each individual subject with detectable response to the visual stimulus (see Methods). The proportion of voxels meeting criteria for visual response was smaller in CAA than control subjects (Table 3). Even when restricting to this subset of responsive tissue, the CAA subjects again showed significantly reduced amplitude and prolonged time to peak and baseline (Table 3), also independent of age, sex, hypertension, and use of antihypertensive agent in multivariable analysis. This subset of tissue additionally demonstrated reduced undershoot of baseline in CAA relative to control. In a further secondary analysis to eliminate possible effects of hemorrhage products on changes in the EPI signal, we found essentially identical differences between CAA and controls when excluding all voxels containing microbleeds on co-registered T2*-weighted MR images (data not shown).

We analyzed the 25 CAA subjects for correlations between measurements of ischemic burden (normalized volume of white matter T2-hyperintensity, nWMH) and hemorrhagic burden (number of microbleeds) versus the three fMRI parameters that differed from controls (time-to-peak, time-to-baseline, and amplitude). Longer time to peak response demonstrated moderate correlation with nWMH (Fig. 3, $R=0.53$, $p=0.007$) and remained independent of age, sex, hypertension, and use of antihypertensive agent in multivariable analysis. Similar associations were present in secondary analyses excluding nonresponsive or microbleed-containing voxels. None of the measures of vascular reactivity correlated with number of microbleeds.

Resting absolute CBF for the visually activated ROI was measured by ASL in 22 CAA subjects and the 12 controls. This analysis showed was no difference between resting CBF in CAA vs control in univariate (44.0 ± 12.6 vs 45.0 ± 10.0 ml/100g/min, $p=0.8$) or multivariable models. Similar results were obtained when the analysis excluded unresponsive voxels or voxels containing microbleeds.

Discussion

This first reported application of fMRI analysis to subjects with advanced CAA demonstrates impaired vascular reactivity to physiologic stimulation relative to similar aged control subjects. The response to visual stimulation in CAA had both reduced amplitude and altered timing, with slower ascent to peak and return to baseline. The absolute resting blood flow in visual cortex, conversely, was similar in CAA and control subjects, and similar as well to previously reported values for occipital cortex of healthy individuals over age 60.[23] Variations in baseline CBF can potentially alter the hemodynamic response;[24] the absence

of a baseline CBF difference between the groups therefore also helps support the validity of the observed differences in the transient responses to stimulation.

The results suggest that the major impact of advanced CAA on small vessel function may be to alter the dynamic response to changes in local metabolic demand rather than the resting blood flow. Similar impairments in vascular reactivity have been reported in transgenic mouse models of CAA,[10–12] though it has been difficult to determine whether they reflect the effects of soluble ß-amyloid peptide[25] versus the ß-amyloid deposits in the vessel walls. One study of Tg2576 transgenic mice found that acute depletion of soluble ß-amyloid with a γ-secretase inhibitor restored normal vasoreactivity for vessels with mild (≤20%) but not advanced (>20%) amyloid deposition,[12] suggesting that both soluble and deposited amyloid may participate in the observed physiologic impairment. Interestingly, resting vessel diameters in this study were similar in Tg2576 and wild-type mice,[12] perhaps analogous to the current finding of differences in vascular reactivity but not resting blood flow between CAA and controls.

CAA-associated delays in response to physiologic stimulation were suggested by a prior analysis using fTCD,[13] and in the current study, appear to be at least as robust as the reductions of response amplitude. Prolonged time-to-peak response correlated with greater volume of white matter hyperintensities within the CAA group, raising the possibility that the timing of the vascular response might contribute to maintaining adequate blood flow and avoiding chronic ischemic injury. If confirmed, this finding would suggest that vascular reactivity to visual stimulation (presumably reflecting the effects of CAA within visual cortex) may act as a reasonably accurate marker of overall CAA burden throughout the brain, thus explaining the correlation with total brain WMH burden.

The BOLD response depends on the complex process of neurovascular coupling[26] and indeed is widely used to identify patterns of neuronal rather than vascular activation. One important limitation to our analysis is therefore that altered response to physiologic stimulation in CAA might reflect tissue damage rather than true vascular dysfunction. It is reassuring in this regard that secondary analysis excluding unresponsive voxels (potentially representing sites of unrecognized neuronal injury) yielded essentially the same findings as analysis of the full ROI. Excluding unresponsive voxels may in fact bias towards the null result, as some or all of these unresponsive sites might actually reflect severe vascular damage rather than tissue injury (and this analysis indeed excluded more voxels in CAA than control subjects; Table 3). It is similarly reassuring that excluding all hemorrhage-containing voxels also had no substantial effect on the findings, suggesting that the results were not caused by possible T2*-effects of chronic blood products on the EPI signal. Another notable limitation is that our approach measures vascular reactivity only in visually activated cortex rather than the brain as a whole. We chose to focus on visual stimulation because of the robust response elicited by this stimulus and the tendency for CAA to be most severe in occipital brain regions.[15–17] We also note that fMRI at 1.5T has a lower time-series signal-to-noise ratio compared to higher field strengths,[27] though the effect of reduced detection power at 1.5T would again be expected to bias towards a null result rather than positive findings. Another potential bias towards a null result would be varying use by study subjects of vasoactive ingestibles such as caffeine, which we did not measure in the current study.

The current data indicate that the vascular effects of advanced CAA are robustly detectable using fMRI. One strength of fMRI is that unlike fTCD,[13, 14] it provides anatomic information on the location of altered vascular reactivity. The current results thus point to the potential for multimodal imaging-based approaches to untangle the spatial

interrelationship between the locations of CAA,[16, 17] impaired vascular reactivity, and CAA-related foci of tissue injury.[1–5]

Supplementary Material

Refer to Web version on PubMed Central for supplementary material.

Acknowledgments

This work was supported by grants from the National Institutes of Health (2R01 AG026484, R01 NS070834) and was carried out at the Athinoula A.Martinos Center for Biomedical Imaging at the Massachusetts General Hospital, using resources provided by the Center for Functional Neuroimaging Technologies, P41RR14075, a P41 Regional Resource supported by the Biomedical Technology Program of the NIH National Center for Research Resources.

References

1. Okazaki H, Reagan TJ, Campbell RJ. Clinicopathologic studies of primary cerebral amyloid angiopathy. Mayo Clin. Proc. 1979; 54:22–31. [PubMed: 759733]
2. Kimberly WT, Gilson A, Rost NS, Rosand J, Viswanathan A, Smith EE, Greenberg SM. Silent ischemic infarcts are associated with hemorrhage burden in cerebral amyloid angiopathy. Neurology. 2009; 72:1230–1235. [PubMed: 19349602]
3. Menon RS, Kidwell CS. Neuroimaging demonstration of evolving small vessel ischemic injury in cerebral amyloid angiopathy. Stroke. 2009; 40:e675–677. [PubMed: 19850897]
4. Soontornniyomkij V, Lynch MD, Mermash S, Pomakian J, Badkoobehi H, Clare R, Vinters HV. Cerebral microinfarcts associated with severe cerebral beta-amyloid angiopathy. Brain Pathol. 2010; 20:459–467. [PubMed: 19725828]
5. Gregoire SM, Charidimou A, Gadapa N, Dolan E, Antoun N, Peeters A, Vandermeeren Y, Laloux P, Baron JC, Jager HR, Werring DJ. Acute ischaemic brain lesions in intracerebral haemorrhage: multicentre cross-sectional magnetic resonance imaging study. Brain : a journal of neurology. 2011; 134:2376–2386. [PubMed: 21841203]
6. Haglund M, Englund E. Cerebral amyloid angiopathy, white matter lesions and Alzheimer encephalopathy - a histopathological assessment. Dement Geriatr Cogn Disord. 2002; 14:161–166. [PubMed: 12218260]
7. Gurol ME, Irizarry MC, Smith EE, Raju S, Diaz-Arrastia R, Bottiglieri T, Rosand J, Growdon JH, Greenberg SM. Plasma beta-amyloid and white matter lesions in AD, MCI, and cerebral amyloid angiopathy. Neurology. 2006; 66:23–29. [PubMed: 16401840]
8. Salat DH, Smith EE, Tuch DS, Benner T, Pappu V, Schwab KM, Gurol ME, Rosas HD, Rosand J, Greenberg SM. White matter alterations in cerebral amyloid angiopathy measured by diffusion tensor imaging. Stroke. 2006; 37:1759–1764. [PubMed: 16763176]
9. Arvanitakis Z, Leurgans SE, Wang Z, Wilson RS, Bennett DA, Schneider JA. Cerebral amyloid angiopathy pathology and cognitive domains in older persons. Ann. Neurol. 2011; 69:320–327. [PubMed: 21387377]
10. Park L, Anrather J, Forster C, Kazama K, Carlson GA, Iadecola C. Abeta-induced vascular oxidative stress and attenuation of functional hyperemia in mouse somatosensory cortex. J Cereb Blood Flow Metab. 2004; 24:334–342. [PubMed: 15091114]
11. Shin HK, Jones PB, Garcia-Alloza M, Borrelli L, Greenberg SM, Bacskai BJ, Frosch MP, Hyman BT, Moskowitz MA, Ayata C. Age-dependent cerebrovascular dysfunction in a transgenic mouse model of cerebral amyloid angiopathy. Brain. 2007; 130:2310–2319. [PubMed: 17638859]
12. Han BH, Zhou ML, Abousaleh F, Brendza RP, Dietrich HH, Koenigsknecht-Talboo J, Cirrito JR, Milner E, Holtzman DM, Zipfel GJ. Cerebrovascular dysfunction in amyloid precursor protein transgenic mice: contribution of soluble and insoluble amyloid-beta peptide, partial restoration via gamma-secretase inhibition. J. Neurosci. 2008; 28:13542–13550. [PubMed: 19074028]
13. Smith EE, Vijayappa M, Lima F, Delgado P, Wendell L, Rosand J, Greenberg SM. Impaired visual evoked flow velocity response in cerebral amyloid angiopathy. Neurology. 2008; 71:1424–1430. [PubMed: 18955685]

14. Menendez-Gonzalez M, Garcia-Garcia J, Calleja S, Rojo J, Ribacoba R. Vasomotor reactivity is similarly impaired in patients with Alzheimer's disease and patients with amyloid hemorrhage. Journal of neuroimaging: official journal of the American Society of Neuroimaging. 2011; 21:e83–85. [PubMed: 19912480]
15. Vinters HV, Gilbert JJ. Cerebral amyloid angiopathy: incidence and complications in the aging brain. II. The distribution of amyloid vascular changes. Stroke. 1983; 14:924–928. [PubMed: 6658996]
16. Johnson KA, Gregas M, Becker JA, Kinnecom C, Salat DH, Moran EK, Smith EE, Rosand J, Rentz DM, Klunk WE, Mathis CA, Price JC, Dekosky ST, Fischman AJ, Greenberg SM. Imaging of amyloid burden and distribution in cerebral amyloid angiopathy. Ann. Neurol. 2007; 62:229–234. [PubMed: 17683091]
17. Ly JV, Donnan GA, Villemagne VL, Zavala JA, Ma H, O'Keefe G, Gong SJ, Gunawan RM, Saunde T, Ackerman U, Tochon-Danguy H, Churilov L, Phan TG, Rowe CC. 11C-PIB binding is increased in patients with cerebral amyloid angiopathy-related hemorrhage. Neurology. 2010; 74:487–493. [PubMed: 20142615]
18. O'Donnell HC, Rosand J, Knudsen KA, Furie KL, Segal AZ, Chiu RI, Ikeda D, Greenberg SM. Apolipoprotein E genotype and the risk of recurrent lobar intracerebral hemorrhage. N. Engl. J. Med. 2000; 342:240–245. [PubMed: 10648765]
19. Knudsen KA, Rosand J, Karluk D, Greenberg SM. Clinical diagnosis of cerebral amyloid angiopathy: Validation of the Boston Criteria. Neurology. 2001; 56:537–539. [PubMed: 11222803]
20. van der Kouwe AJ, Benner T, Salat DH, Fischl B. Brain morphometry with multiecho MPRAGE. Neuroimage. 2008; 40:559–569. [PubMed: 18242102]
21. Greenberg SM, Vernooij MW, Cordonnier C, Viswanathan A, Al-Shahi Salman R, Warach S, Launer LJ, Van Buchem MA, Breteler MM. Cerebral microbleeds: a guide to detection and interpretation. Lancet Neurol. 2009; 8:165–174. [PubMed: 19161908]
22. Greve DN, Fischl B. Accurate and robust brain image alignment using boundary-based registration. Neuroimage. 2009; 48:63–72. [PubMed: 19573611]
23. Chen JJ, Rosas HD, Salat DH. Age-associated reductions in cerebral blood flow are independent from regional atrophy. Neuroimage. 2011; 55:468–478. [PubMed: 21167947]
24. Vazquez AL, Cohen ER, Gulani V, Hernandez-Garcia L, Zheng Y, Lee GR, Kim SG, Grotberg JB, Noll DC. Vascular dynamics and BOLD fMRI: CBF level effects and analysis considerations. Neuroimage. 2006; 32:1642–1655. [PubMed: 16860574]
25. Niwa K, Carlson GA, Iadecola C. Exogenous A beta1-40 reproduces cerebrovascular alterations resulting from amyloid precursor protein overexpression in mice. J Cereb Blood Flow Metab. 2000; 20:1659–1668. [PubMed: 11129782]
26. D'Esposito M, Deouell LY, Gazzaley A. Alterations in the BOLD fMRI signal with ageing and disease: a challenge for neuroimaging. Nature reviews. Neuroscience. 2003; 4:863–872. [PubMed: 14595398]
27. Kruger G, Kastrup A, Glover GH. Neuroimaging at 1.5 T and 3.0 T: comparison of oxygenation-sensitive magnetic resonance imaging. Magnetic resonance in medicine. 2001; 45:595–604. [PubMed: 11283987]

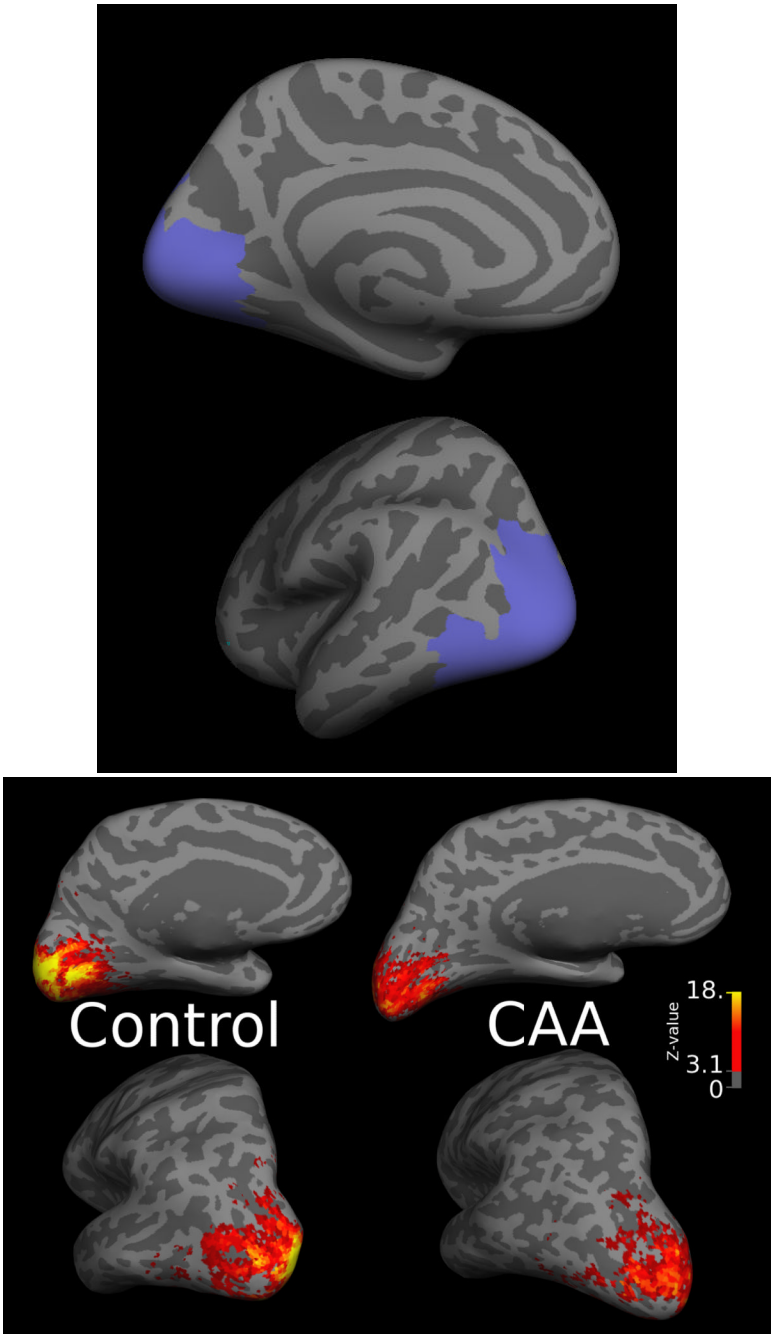

Figure 1.
Visually activated region of interest. Figure 1a shows the functional ROI on the left hemisphere inflated mid-gray cortical surface (darker grayscale values represent sulci). Figure 1b shows functional activation on the inflated mid-gray surface of the left hemispheres of a representative control (left) and CAA (right) subject. The color scale denotes the Z-statistic for activation using the canonical hemodynamic response function (see Methods); Z>3.1 corresponds to the level of significance ($p<0.001$) used to create the functional ROI. There is apparent decreased strength of activation of the CAA subject compared to the control.

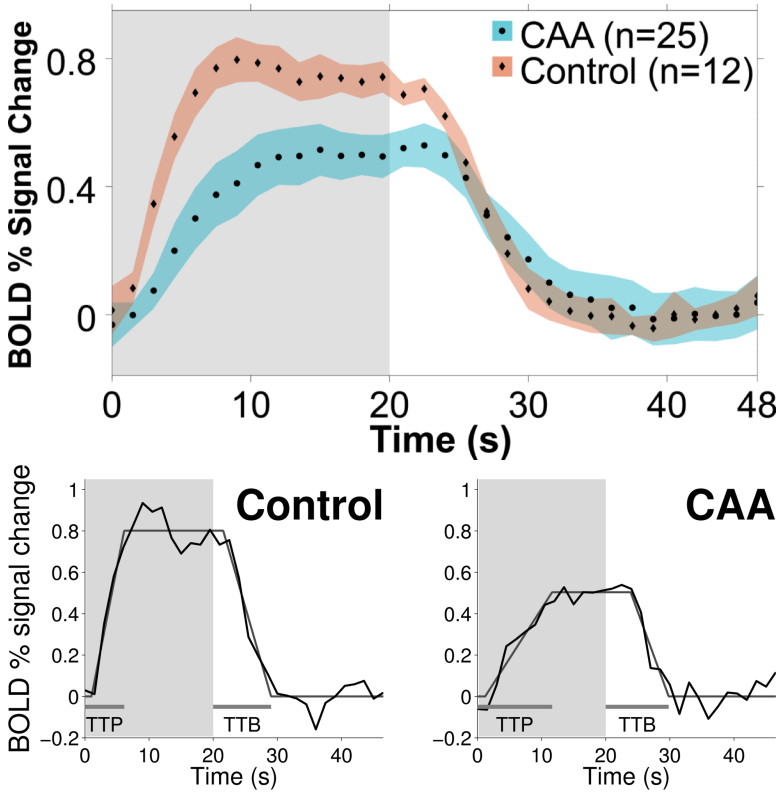

Figure 2.

BOLD response within the functional region of interest. Figure 2a shows average group block responses relative to baseline (set at 0%) for the CAA (blue) and control (red) subjects in the functional ROI. The shaded area denotes the duration of the visual stimulus “on” period for the first 20 seconds of each block. Figure 2b illustrates the trapezoid fits of the representative control (left) and CAA (right) subjects also shown in Figure 1b. Using these fits to measure amplitude, time-to-peak (TTP) response, and time-to-baseline (TTB) response, we found that the CAA subjects had reduced amplitude, prolonged time to peak, and prolonged time to baseline (Table 2).

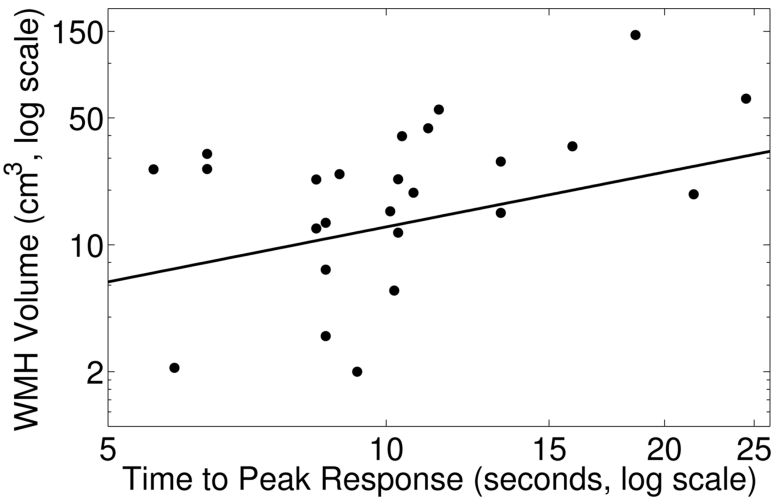

Figure 3.
Association between time to peak response and normalized white matter hyperintensity volume. Values for each CAA subject are plotted on logarithmic scales (Pearson R=0.53, p=0.007).

Table 1

Subject Demographics and Vascular Risk Factors

	CAA (n=25)	Controls (n=12)
Sex, M/F	21/4	8/4
Mean age ± SD, years	70.2 ± 7.8 *	75.3 ± 6.2
Mean MMSE ± SD	27.5 ± 2.5 *	29.2 ± 0.7
HTN, n (%)	16 (64)	4 (33)
DM, n (%)	2 (8)	2 (17)
HL, n (%)	8 (32)	5 (42)
Current tobacco use, n (%)	1 (4)	1 (8)

MMSE = Mini-mental status examination score

HTN = history of hypertension

DM = history of diabetes mellitus

HL = history of hyperlipidemia

* $p<0.05$

Table 2

Vascular Reactivity in Functional Region of Interest

	CAA (n=25)	Controls (n=12)
Time to Peak ± SD, sec	11.1 ± 5.1*	6.4 ± 1.8
Time to Baseline ± SD, sec	16.5 ± 6.7*	11.6 ± 3.1
Amplitude ± SD, % BOLD change	0.65 ± 0.28¶	0.89 ± 0.14
Undershoot ± SD, % BOLD change	0.05 ± 0.12	0.10 ± 0.11

*p<0.001

¶p<0.01

Table 3

Vascular Reactivity Restricted to Activated Voxels

	CAA (n=25)	Controls (n=12)
Responding Voxels ± SD, %	48.1 ± 18.8 *	65.8 ± 9.4
Time to Peak ± SD, sec	11.1 ± 4.7 *	6.6 ± 1.7
Time to Baseline ± SD, sec	16.0 ± 5.9 *	11.0 ± 2.9
Amplitude ± SD, % BOLD change	1.05 ± 0.27 ¶	1.22 ± 0.17
Undershoot ± SD, % BOLD change	0.05 ± 0.13 ¶	0.13 ± 0.08

* $p<0.001$

¶ $p<0.05$